TÜBİTAK

Turkish Journal of Earth Sciences

http://journals.tubitak.gov.tr/earth/

Research Article

Turkish J Earth Sci
(2017) 26: 410-420

doi:10.3906/yer-1706-2

Investigating Moho depth, Curie Point, and heat flow variations of the Yozgat Batholith and its surrounding area, north central Anatolia, Turkey, using gravity and magnetic anomalies

Funda BİLİM*
Department of Geophysical Engineering, Faculty of Engineering, Cumhuriyet University, Sivas, Turkey

Received: 02.06.2017 • **Accepted/Published Online:** 25.10.2017 • **Final Version:** 23.11.2017

Abstract: This paper proposes an interpretation of the Bouguer gravity and magnetic anomaly map of the Yozgat Batholith and its surrounding area (north central Anatolia) for determination of crustal and geothermal structures. In the study area, the Moho and Conrad depths based on a relationship between Bouguer gravity anomaly and seismically determined crustal thickness were estimated as 34–39 km and 19.5–21.5 km, respectively. The crustal thickness of the study area increases from west to east. The estimated Curie point depths in the study area by means of spectral analysis of the magnetic data vary between 10.4 and 19.5 km. The shallow depths indicate that the magnetization is restricted to the upper crust in the study area. In addition, the heat flow values calculated for a thermal conductivity of 2.7 W m^{-1} K^{-1} range from about 80 to 150 mWm^{-2}. The shallow velocity structures in central Anatolia are consistent with the estimated high heat flow values in the upper crust and associated with comparatively high negative Bouguer gravity anomalies.

Key words: Bouguer gravity anomaly map, magnetic anomaly map, Curie point depth, Moho depth, Conrad depth

1. Introduction

The study area is located at the central Anatolian crystalline complex (CACC, proposed by Göncüoğlu et al., 1991) (Figure 1a). The composite Yozgat Batholith (YB) consists of a mostly I-type granitoid association intruding the supra-subduction zone type central Anatolian ophiolite and medium to high-grade metasedimentary rocks of the CACC (Boztuğ et al., 2007). The Bouguer gravity and magnetic anomalies mainly reflect the surface geology (Figure 1b).

In central Anatolia, some gravity, magnetic, and seismological studies have been performed to interpret the crustal structure (Saunders et al., 1998; Ateş et al., 1999, 2005; Aydın et al., 2005; Çakır and Erduran, 2011; Tezel et al., 2013; Kind et al., 2015). Tezel et al. (2013) determined the crustal thickness in the central Anatolia to be 31–38 km determined by receiver function. Although Saunders et al. (1998) and Çakır and Erduran (2011) found it to be about 38 km beneath central Anatolia, Kind et al. (2015) determined the Moho depths to vary between 25 and 40 km by receiver function.

Ateş et al. (1999) analyzed the gravity and aeromagnetic anomalies of Turkey and showed that central Anatolia reflected relatively high-amplitude magnetic anomalies and intense negative gravity anomalies. Aydın et al. (2005) prepared the Curie point depth map of Turkey from magnetic data using a spectral analysis method. Although Ateş et al. (2005) computed the Curie point depths between 7.9 and 22.6 km in central Anatolia, Aydın et al. (2005) found average the Curie point depth as about 20 km.

The main objectives of the present study were to determine the Moho and Conrad depths from the Bouguer gravity data, to assess the interactions between surface geology and magnetic anomalies, and to produce Curie point depth and heat flow maps from magnetic data. In addition, the shapes and locations of deep-seated magnetized sources were presented using an analytic signal (AS).

2. Geological settings

The CACC developed in a context of closure of the Neotethyan Ocean and is composed of high-grade metamorphic rocks, supra-subduction-type ophiolites, and felsic and mafic magmatic rocks. In addition, the CACC is the largest metamorphic domain exposed in Turkey and is surrounded by Neotethyan suture zones formed during subduction and collision of the Eurasian Plate and the Tauride–Anatolide Platform in the Late Cretaceous to Eocene (Şengör and Yılmaz, 1981). This collision between the Eurasian Plate and Tauride–Anatolide Platform

* Correspondence: fbilim@cumhuriyet.edu.tr

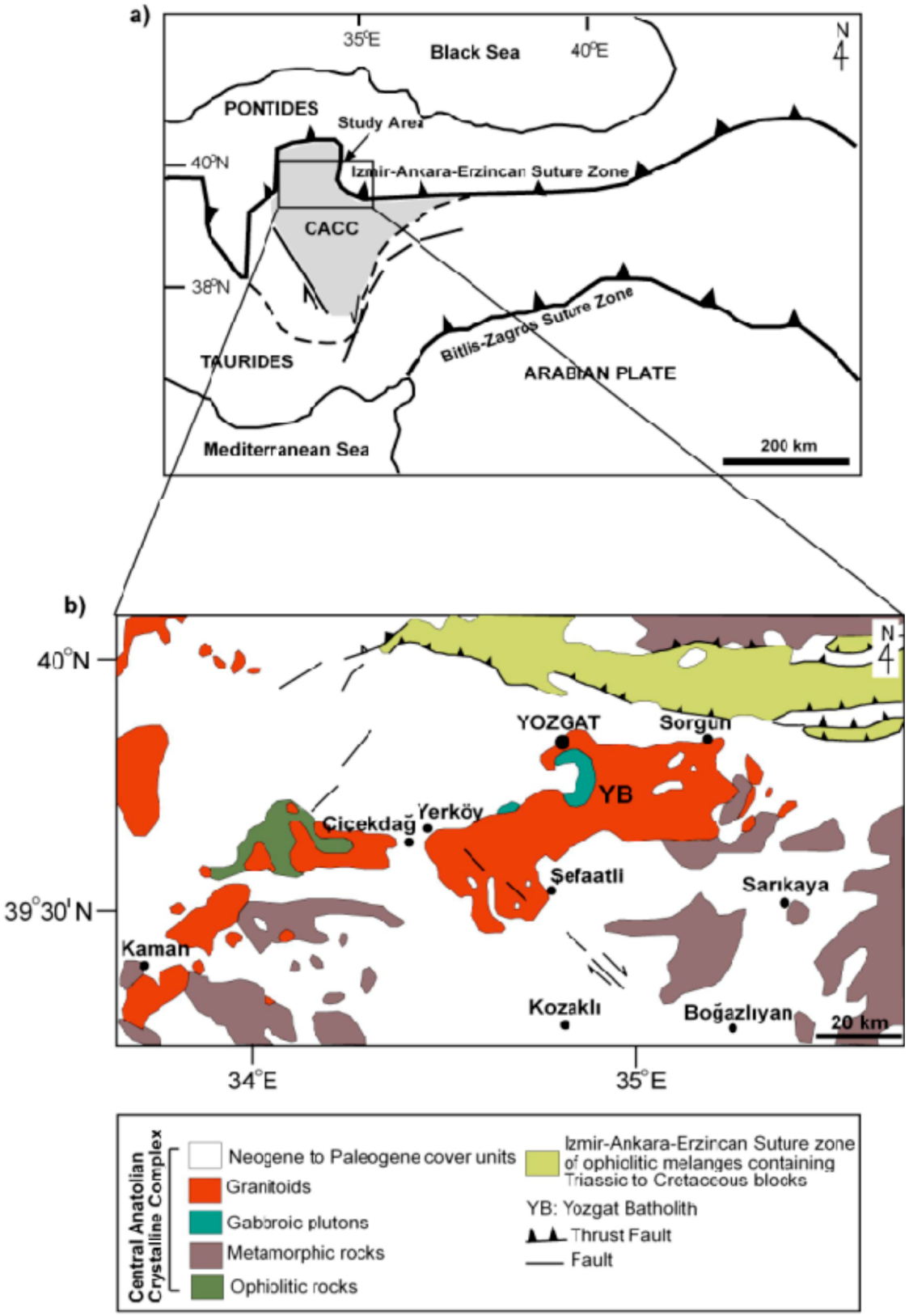

Figure 1. a) The major tectonic divisions in Anatolia-Turkey (modified from Bozkurt and Mittwede, 2005). CACC: Central Anatolian Crystalline Complex; b) Simplified geological map of the study area (modified from Bingöl, 1989).

occurred following consumption (northward subduction) of oceanic crust from the northern branch of the Neotethys along the İzmir–Ankara–Erzincan suture zone (Şengör and Yılmaz, 1981).

The study area is encompassed by the YB within the north of the CACC. The YB is the biggest one in the postcollisional central Anatolian granitoid magmatism (Boztuğ, 1998; Boztuğ et al., 1998; Erler and Göncüoğlu, 1996) (Figure 1). The north of the YB is bounded on the İzmir-Ankara-Erzincan Suture Zone (Figure 1a). A surface geological map of the study area is presented in Figure 1b. There are wide outcrops of granitoids of the CACC and ophiolitic remnants of the northern branch of the Neotethys and the CACC. Paleozoic–Mesozoic aged metamorphic rocks located in the south of the study area were obducted by ophiolitic rocks and both are intruded by granitoids. The crustal metamorphic rocks consist of amphibolites, gneisses, schists, and marbles of the CACC. These units are covered by Neogene–Paleocene sedimentary and volcanic rocks (Figure 1b). The composite YB includes mainly the postcollisional high-K calc-alkaline, I type granitoid units. I-type granitoids of the composite YB have porphyritic textures with large K-feldspar and plagioclase megacrysts (Boztuğ et al., 2009). Boztuğ and Harlavan (2008) suggested that the K-Ar cooling ages of the S-I-A type granites in central Anatolia range from 80 Ma to 65 Ma. Boztuğ et al. (2009) propose that the amphibole and biotite K-Ar and ^{40}Ar-^{39}Ar ages of individual central Anatolia granitoids suggest rapid cooling from 500 °C to 300 °C and this rapid cooling could indicate shallow emplacement and rapid conductive cooling or rapid exhumation from a midcrustal level. According to Boztuğ et al. (2007), there are both mafic and hybridizated felsic I-type granites derived from the solidification of coeval mafic and felsic magma sources, respectively. In addition, all the I-type granitoids of the YB are thought to have been inherited from a metasomatized mantle and mafic lower crustal sources, as well as from magma–crust interaction by Boztuğ et al. (2007).

3. Methodology

3.1. Gravity and magnetic anomalies of the study area

The Bouguer gravity and magnetic data were provided by the General Directorate of Mineral Research and Exploration (MTA) of Turkey. The Bouguer gravity anomaly map of the study area mainly reflects the general geologic structure of the surface and subsurface (Figure 2). The anomaly is negative with values ranging from mainly –30 to –95 mGal with a west to east trend. Figure 2 shows three negative anomalies in the study area: 1) A high negative gravity anomaly closure (–40 mGal) located in the west of the study area is caused by the ophiolitic rocks and granitoids the majority of which may be hidden beneath Neogene to Paleogene cover units (Figure 1b); 2)

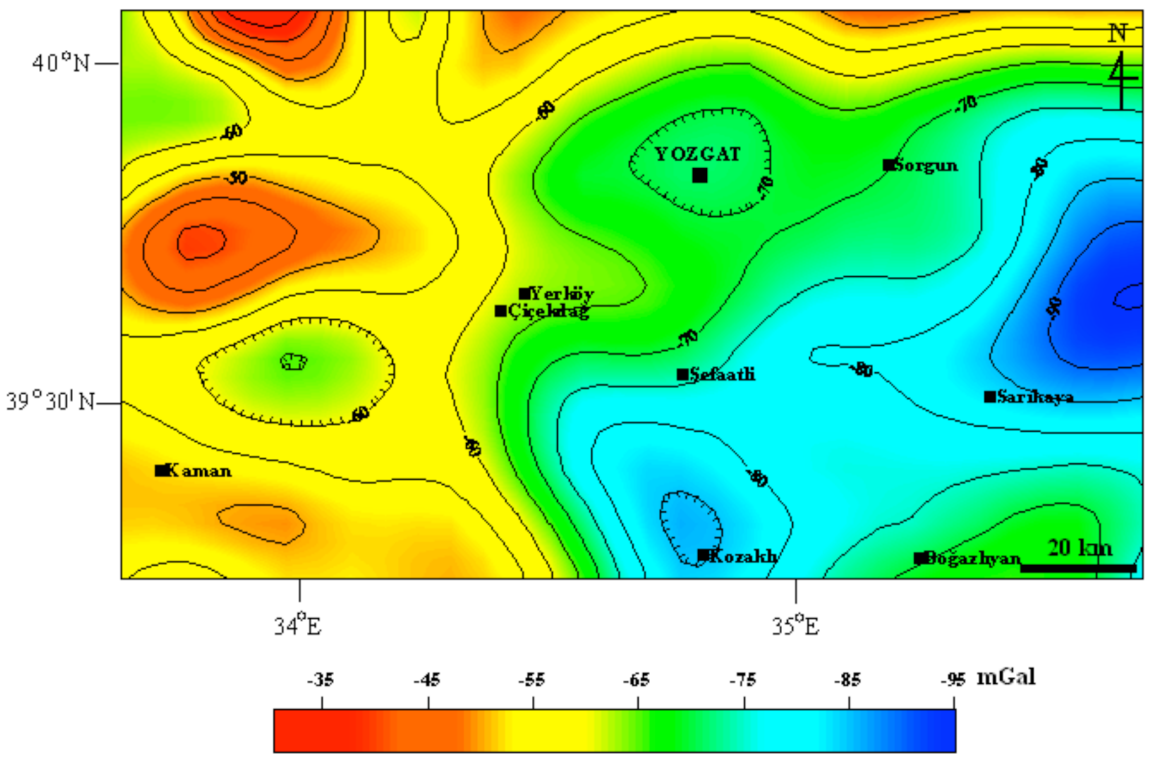

Figure 2. The Bouguer gravity anomaly map of the study area. The contour interval is 50 nT.

Medium gravity anomalies ranging from –60 to –70 mGal with a northeast to southwest trend situated at the YB may be associated with the granitoids of the composite YB; 3) The very low amplitude gravity anomaly (–95 mGal) is located around the town of Sarıkaya. These low gravity values do not reflect the metamorphic outcrops located in the SE corner of the study area (Figures 1b and 2), and thus may be associated with hot thermal structures in the upper crust. The towns of Sorgun and Sarıkaya include two hot springs. Temperatures of the hot springs in Sorgun and Sarıkaya are 50–61 °C and 46–48 °C, respectively (Erişen et al., 1996).

Figure 3a shows the total field residual aeromagnetic anomaly data. The flight line of aircraft is 600 m from the ground's surface. Generally, the anomalies are in harmony with surface geology. The magnetic anomalies mainly range from –250 to +450 nT. The W–E trending intense anomaly (Figure 3a) can be mainly related to the composite YB consisting of a granitoid association intruding the supra-subduction zone-type central Anatolian ophiolite and medium-to high-grade metasedimentary rocks of the CACC (Boztuğ et al., 2007). The NW–SW trending short wavelength magnetic anomalies between the town of Şefaatli and the town of Sorgun are most likely associated with metamorphic rocks.

3.2. Moho depth estimation from gravity data

Moho depth can be estimated from gravity anomaly data. The relationship between Bouguer gravity anomaly and seismically determined crustal thickness revealed that they are linearly related, indicating that isostasy prevails on a regional scale (Woolard, 1959; Riad et al., 1981; Ram Babu, 1997). Woolard (1959) and Ram Babu (1997) give the empirical relationships between Bouguer anomaly and crustal thickness for whole earth as follows:

$$H=32-0.08\Delta g \quad (1)$$

and

$$H_c=18.6-0.031\Delta g \quad (2)$$

where Δg is gravity anomaly, H is the Moho depth and H_c is the Conrad depth.

Riad et al. (1981) proposed the other empirical relationships to estimate the Moho depth from gravity data as follows:

$$H=29.98-0.0075\Delta g \quad (3)$$

Recently, these relationships have been applied successfully by several authors to gravity data (e.g., Rivero et al., 2002; Ateş et al., 2012; Maden et al., 2015). In the present study, the Moho and Conrad depths of the study area were estimated from Eqs. (1) and (3) (Figures 4a and 4b) and Eq. (2) (Figure 4c), respectively.

3.3. Determination of Curie point depth, thermal gradient, and heat flow

The well-known method given by Okubo et al. (1985) was used in the determination of Curie point depth (CPD) from aeromagnetic anomaly data. This method was previously used by many authors (i.e. Okubo et al., 1985, 1989; Tsokas et al., 1998; Bilim, 2007, 2011; Aboud et al., 2011; Karastathis et al., 2011; Obande et al., 2014; Hsieh et al., 2014). The bottom depth of the magnetic Earth's crust is generally accepted to be related to CPD. To determine the CPD, firstly reduction to the pole (RTP), which removes the distortion caused by the Earth's magnetic field, was applied to the total field residual aeromagnetic anomaly data of the study area (Figure 3b). The declination and inclination angles of the Earth's magnetic field were taken as 4°E and 55°N, respectively, in the RTP processes. Secondly, the radially averaged power spectrum of the RTP data was calculated. Then the depth to the centroid (z_0) and the top depth of the magnetic sources (z_t) were estimated. Finally, the Curie depth (z_b) was calculated by $z_b=2z_0-z_t$.

The RTP anomaly map applied to the residual total field aeromagnetic anomaly data was subdivided into 3 blocks (N1, N2, and N3 indicate the center of the blocks) for spectral analysis (Figure 3b). Nwobgo (1998) suggested that the grid size must be at least four or six times of the depth of the magnetic sources. El-Nabi (2012) suggested also that the window size of 60 km × 60 km was necessary to obtain the Curie point estimate from magnetic data. Ateş et al. (2005) calculated the average CPD as 15.36 km in central Anatolia. Therefore, the study area was divided into 3 overlapping blocks with dimensions 60 km × 60 km. The estimated CPDs are given in Table 1. As an example, a plot of the spectral analysis of the block N3 is given in Figures 5a and 5b. Figure 6a shows the estimated CPD map of the study area. B23, B24, and B25 were taken from Ateş et al. (2005). N1, N2, and N3 are newly calculated CPDs in this study (Figure 6a; Table 1).

The AS of RTP magnetic data was computed to understand the distribution of magnetic sources and correlate the CPDs in the study area (black-white (gray image) map inserted in Figure 6). The amplitude of the AS is defined as the square root of the squared sum of the vertical and two horizontal derivatives of the magnetic field (Roest et al., 1992). The AS exhibits maximum amplitudes over magnetization contrast without making assumptions on the direction of source body magnetization.

Curie depth depends upon the Curie temperature, which varies from 350 to 680 °C in magnetic minerals (Piper, 1987). However, Curie point is usually referred to a temperature of 580 °C (Mayhew, 1982; Okuba et al., 1985; Hunt et al., 1995). Lefebvre et al. (2013) determined from paleomagnetic analysis at the CACC that the magnetic carrier of the ChRM in the samples is magnetite, evidenced by maximum unblocking temperatures and fields around 580 °C. Therefore, the thermal gradient values of the study area were estimated using 580 °C from the equation of grad T = 580 °C/Curie depth (Table 1).

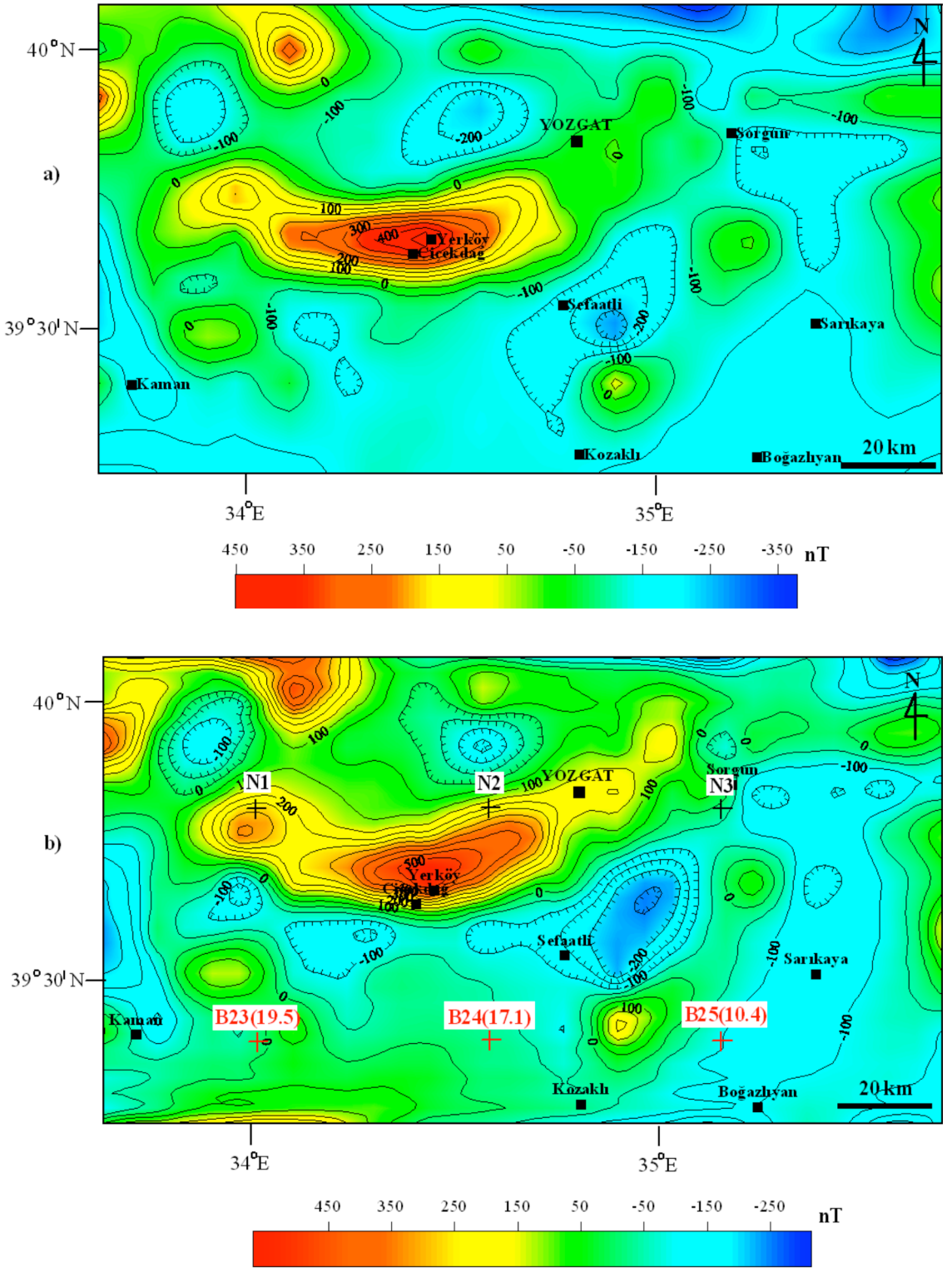

Figure 3. a) The residual magnetic anomaly map of the study area. The contour interval is 50 nT; b) The RTP anomaly map applied to the residual total field aeromagnetic anomaly data. Black plus (+) signs indicate the center of the blocks for using in estimation of CPDs. The block names of B23 to B25 values were taken from Ateş et al. (2005). The block names of N1 to N3 display the new estimated CPDs in this study.

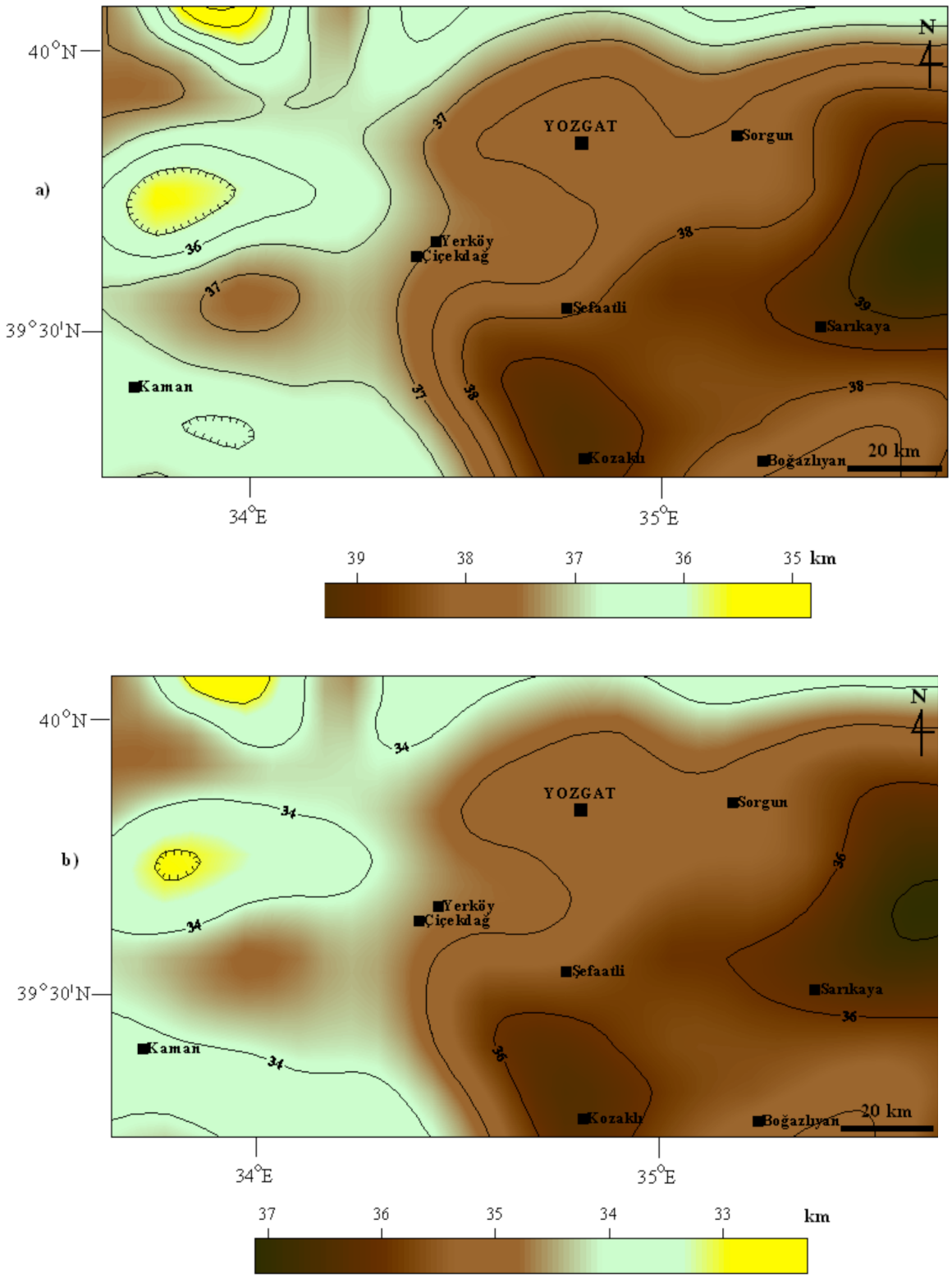

Figure 4. a) Moho depth map of the study area calculated from the gravity anomaly data (Figure 2) by using empirical equations (Woolard, 1959; Ram Babu, 1997). Contour interval is 0.5 km. Contour interval is 0.3 km; b) Moho depth map of the study area calculated from the gravity anomaly data (Figure 2) by using empirical equations (Riad et al., 1981). Contour interval is 0.5 km; c) Conrad depth map of the study area calculated from the gravity anomaly data (Figure 2) by using empirical equations (Woolard, 1959; Ram Babu, 1997).

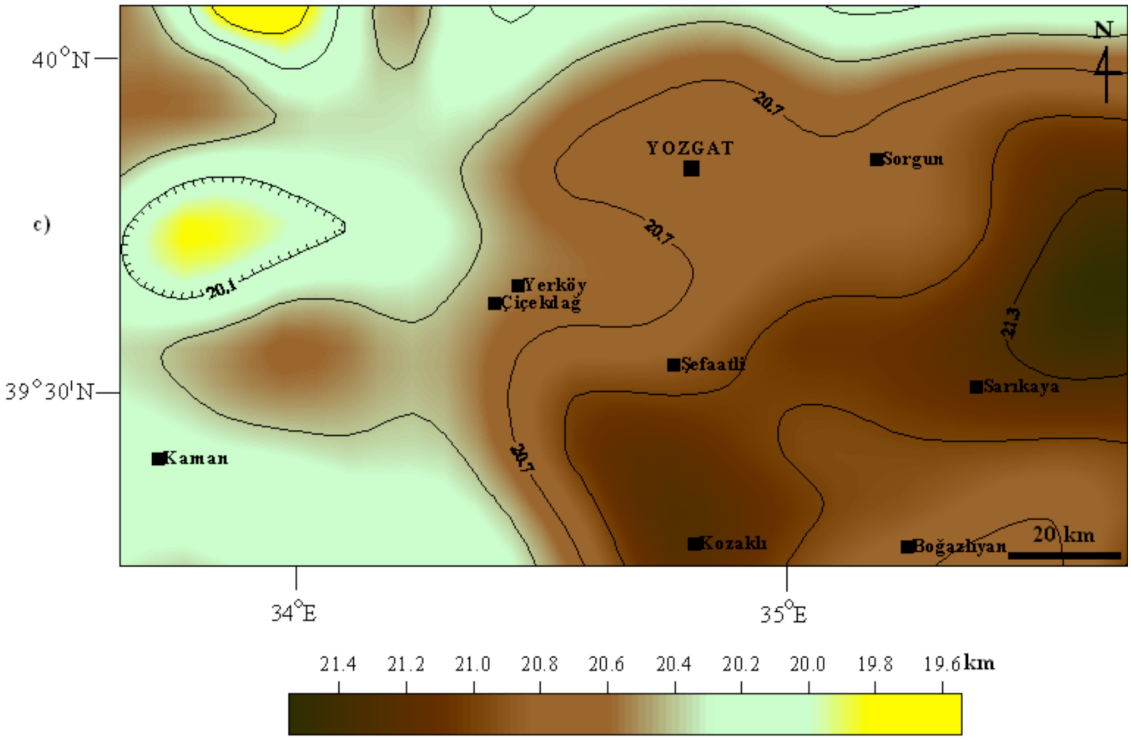

Figure 4. (Continued).

The surface heat-flow can be estimated from the equation of

$$q_{00} = -k\frac{\partial T}{\partial z}$$

where q_0 is the surface heat-flow, $\frac{\partial T}{\partial z}$ is the thermal gradient (grad T), and k = k(z) is the thermal conductivity as a function of depth (z) (Turcotte and Schubert, 1982; Artemieva and Money, 2001). In the present study, the heat flow map of the study area (Figure 6b) was produced for the thermal conductivity value of 2.7 mW/m^2 (for the upper crust, Springer, 1999).

4. Discussion and conclusion

In the present study, Moho and Conrad depths were estimated from Bouguer gravity data for the first time in the study area. I employed Eqs. (1) and (3) suggested by Woolard (1959) and Riad et al. (1981), respectively, to estimate the Moho depth. In addition, I applied Eq. (2) suggested by Woolard (1959) to estimate the Conrad depth. The estimated thickness of the crust varies from about 34 km to 39 km in the study area from Eq. (1) (Figure 4a). By using Eq. (3), the Moho depth map was also produced for the study area (Figure 4b). The estimated Moho depths vary from 32.5 km to 38 km (Figure 4b). Figure 4c shows the estimated Conrad depth map of the study area. The

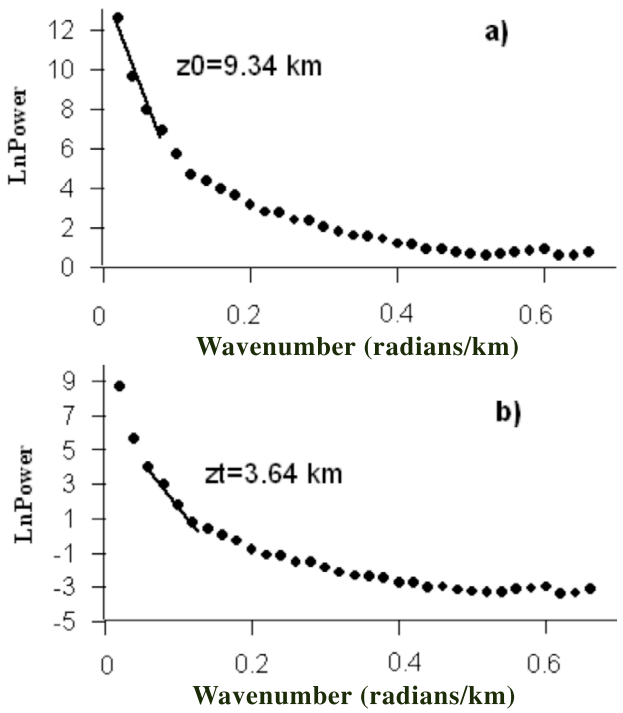

Figure 5. Spectral analysis for block number N3 for the RTP anomaly map. a) estimated depth to centroid, z_0; b) estimated depth to z_t (top boundary of magnetic layer). Solid lines represent the least-square fit of the power spectra.

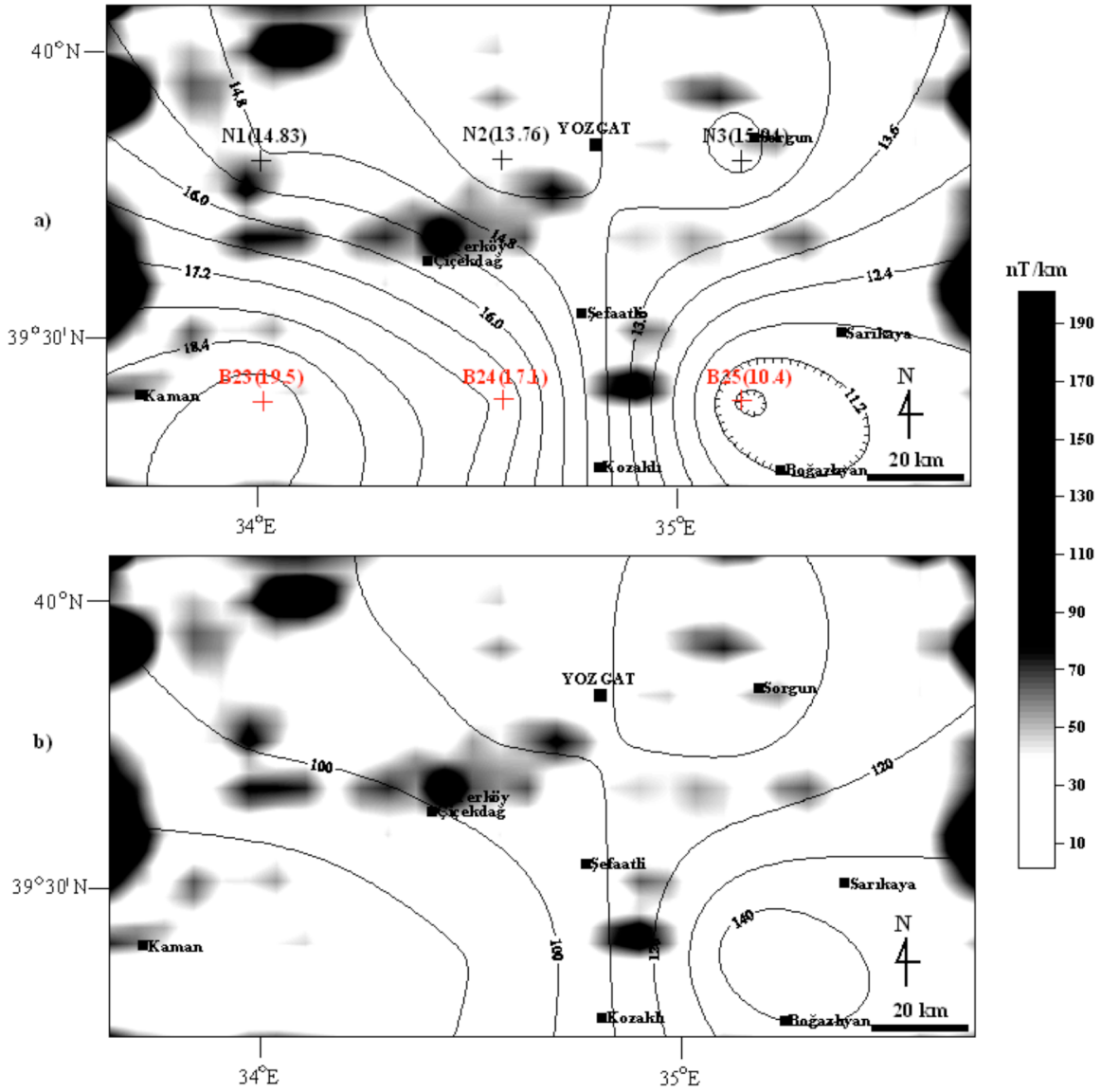

Figure 6. a) The estimated Curie point depths map from the reduced-to-pole (RTP) magnetic anomaly map of the study area. CPDs are below the sea level and contour interval is 0.6 km. Plus (+) signs indicate the center of the blocks for using in estimation of CPDs. The block names of B23 to B25 values were taken from Ateş et al. (2005). The block names of N1 to N3 display the new estimated CPDs in this study. The black and white (gray image) map shows the analytic signal (AS) map applied to reduction to the pole anomaly data (Figure 3b) applied to the residual total field magnetic anomaly map (Figure 3a). b) Heat-flow maps of the study area for thermal 2.7 W m^{-1} K^{-1}. Contour interval is 10 mW m^{-2}. The black and white (gray image) map shows the AS map applied to the reduction to the pole anomaly data (Figure 3b) applied to the residual total field magnetic anomaly map (Figure 3a).

Conrad depths range between 19.5 km and 21.5 km. The Moho maps (Figures 4a and 4b) assumed that the mantle occurs at a much greater depth in the east of the study region than in the west of the study area. The average thickness of the crust is determined as about 37 km in this study. These Moho depths, estimated from both the equation of Wollard (1959) and the equation of Riad et al. (1981), are more consistent with the more recent studies performed in central Anatolia by Tezel et al. (2013) and Kind et al. (2015). Tezel et al. (2013) defined the Moho depth and uppermost mantle shear-wave speed as varying between 31 km and 38 km, between 4 km s^{-1} and 4.3 km s^{-1}, respectively, in central Anatolia by receiver technique applied to 120 broadband seismic stations. Kind et al. (2015) calculated the thickness of the lithosphere and Moho depths beneath Turkey from S-receiver function and suggested that the lithosphere

Table 1. Estimated CPDs, geothermal gradients, and heat-flow values in the study area.

The centers of the blocks	Curie point depth (z_b)km	Geothermal gradient (°C/km)	Heat flow (mW/m^{-2}) k = 2.7 W m^{-1} K^{-1}
N1	14.83	39.16	105.73
N2	13.76	42.15	113.80
N3	15.04	38.56	104.11
B23[1]	19.50[1]	29.74	80.29
B24[1]	17.10[1]	33.91	91.55
B25[1]	10.40[1]	55.77	150.57

[[1]Ateş et al., 2005]

thickness and the Moho depths beneath the entire region of Anatolia vary between 80 km and 100 km and between 25 km and 40 km, respectively. Significant seismological studies to determine the Moho depths in central Anatolia are given in Table 2. Crustal density decreases from west to north in the study area, while the crustal thickness and heat flow increase gradually to about 39 km and 145 mWm^{-2}, respectively (Figures 2, 4, and 6b).

I estimated the Curie point depths to vary between 10.4 and 19.5 km (Table 1; Figure 6a). Shallow depths indicate that the magnetization is restricted to the upper crust in the study area. The estimated CPDs are also consistent with the result given by Boztuğ et al. (2007, 2009), who suggested that the composite YB has mid-crustral emplacement depths ranging from 7 to 13 km (2 to 4 kbar) from geothermobarometric studies conducted in various central Anatolia granitoids derived from different hybrid magmas. The source magmas were likely derived from crustal and enriched lithospheric mantle sources that were melted nearly contemporaneously in the postcollisional extensional-related geodynamic setting of Late Cretaceous Anatolia (Boztuğ and Arehart, 2007). The estimated CPDs are not consistent with the results published by Aydın et al. (2005). While the CPDs values determined by Aydın et al. (2005) increase toward the east and southeast of Yozgat (>20 km), the CPD values determined in this study decrease to 11–10 km in close harmony with the geothermal area located east and southeast of Yozgat (temperatures of hot springs in the towns of Sorgun and Sarıkaya are 50–61 °C and 46–48 °C, respectively (Erişen et al., 1996)).

The estimated geothermal gradient (Table 1) and heat flow values (Figure 6b) of the YB and its surroundings area range from 29.74 to 55.77 °C and from 80.29 to 150.57 mWm^{-2}, respectively. The distributions of magnetic sources obtained from the AS process may be mainly associated with the granitoid rocks of the YB in the study area (Figure 6). The magnetic sources (except for south of Şefaatli) are not seen in the south of the study area, which is covered by young cover unit and metamorphic rocks (Figures 1b and 6). The NE–SW trending two magnetic sources in the south of Şefaatli may be associated with elliptical granitoids beneath the cover units (Figures 1b and 6). The weak magnetic anomalies (Figure 3) between Sorgun, Sarıkaya, and Boğazlıyan may be associated with hot thermal structures characterized by high heat flow value (>140 mWm^{-2}), shallow CPD (about 10 km), and moderate temperatures of hot springs (about 46–60 °C in Sorgun and Sarıkaya (Erişen et al., 1996)).

The locations of epicenters and magnitudes (>3.0) of earthquakes that occurred in the study area between 1900 and 2015 are given in Figure 7. The earthquake data set was taken from the catalogue of the General Directorate

Table 2. Significant Moho depth calculation in central Anatolia.

Crustal thickness (Moho depth)-km	Method	References
38	Receiver functions	Saunders et al. (1998)
38	P and S-wave receiver function	Çakır and Erduran (2011)
31–38	Receiver functions	Tezel et al. (2013)
25–40	S-receiver function	Kind et al. (2015)
37	The relationship between Bouguer gravity anomaly and seismically determined crustal thickness	This study

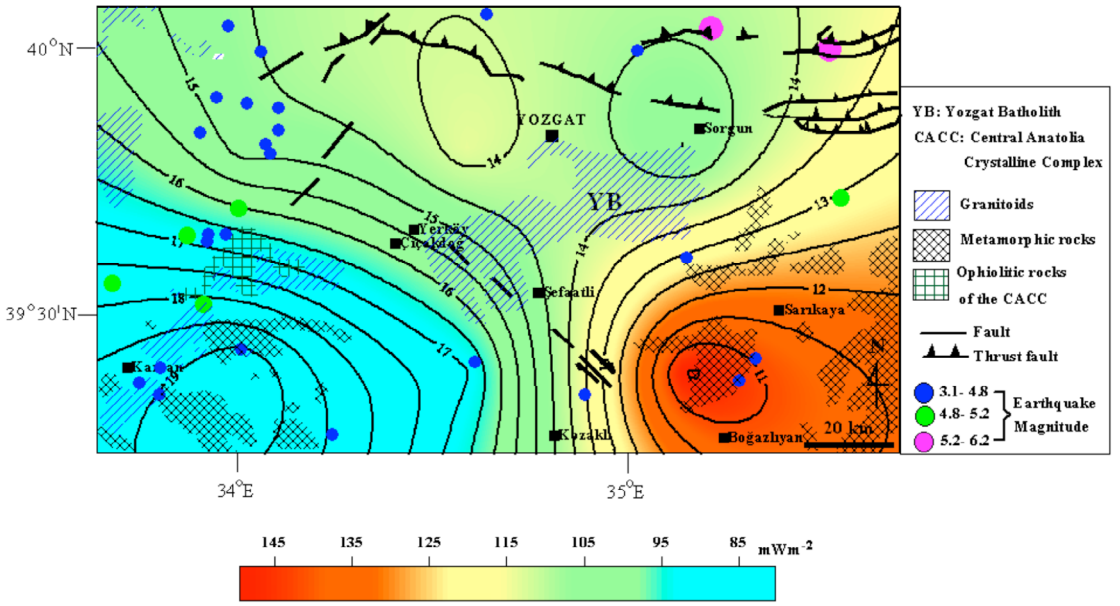

Figure 7. Seismicity of the study area for 1900–2015 (taken from the catalogue of the General Directorate of Disaster Affairs of Turkey). The Curie point depths contours (contour interval is 0.5 km), general geologic units, and heat flow map are inserted for comparison.

of Disaster Affairs of Turkey. Figure 7 shows that the study area is not seismically active and locations of the epicenters of earthquake are distributed mainly in the west and north of the study area related to the surface faults. In addition, there are some seismic activities in the SW of Sarıkaya, where the highest heat flow contour was determined in this study (Figure 7). High heat flow regions usually have low Vpvelocities. Al-Lazki et al. (2004) estimated low Pn velocity zones (<7.9 km s^{-1}) by using the P-wave traveltime inversion method beneath central Anatolia that may be as a result of an anomalously hot and/or thin mantle lid. The shallow velocity structures in central Anatolia are consistent with the estimated high heat flow values in the upper crust and associated with comparatively high negative Bouguer gravity anomalies.

Acknowledgments

The author thanks the General Directorate of the Mineral Research and Exploration (MTA) of Turkey for gravity and aeromagnetic data. The author is also grateful for the efforts made by the editor and the reviewers, which made a considerable contribution to the paper.

References

Aboud E, Salem A, Mekkawi M (2011). Curie depth map for Sinai Peninsula, Egypt deduced from the analysis of magnetic data. Tectonophysics 506: 46-54.

Al-Lazki A, Sansvol E, Şeber D., Barazangi M, Turkelli N, Mohamad R (2004). Pn tomographic imaging of mantle lid velocity and anisotropy at the junction of the Arabian, Eurasian and African plates. Geophys J Int 158: 1024-1040.

Artemieva IM, Mooney WD (2001). Thermal thickness and evolution of Precambrian lithosphere: a global study. J Geophys Res 106: 16387-16414.

Ateş A, Kearey P, Tufan S (1999). New gravity and magnetic maps of Turkey. Geophys J Int 136: 499-502.

Ateş A, Bilim F, Büyüksaraç A (2005). Curie point depth investigation of Central Anatolia, Turkey. Pure Appl Geophys 162: 357-371.

Ateş A, Bilim F, Büyüksaraç A, Aydemir A, Bektaş O, Aslan Y (2012). Crustal structure of the Turkey from aeromagnetic, gravity and deep seismic reflection data. Surv Geophys 33: 869-885.

Aydın I, Karat HI, Koçak A (2005). Curie-point depth map of Turkey. Geophys J Int 162: 633-640.

Bilim F (2007). Investigation into the tectonic lineaments and thermal structure of Kutahya-Denizli region, Western Anatolia, from using aeromagnetic, gravity and seismological data. Phys Earth Planet Int 165: 135-146.

Bilim F (2011). Investigation of the Galatian volcanic complex in the northern central Turkey using potential field data. Phys Earth Planet Int 185: 36-43.

Bingöl E (1989). Geological map of Turkey (Scale: 1/2000000). General Directorate of Mineral Research and Exploration (MTA), Ankara, Turkey.

Bozkurt E, Mittwede SK (2005). Introduction: evolution of continental extensional tectonics of western Turkey. Geodinamica Acta 18: 153-165.

Boztuğ D (1998). Post-Collisional central Anatolian alkaline plutonism, Turkey. Turkish J Earth Sci 7: 145-165.

Boztuğ D, Arehart GB (2007). Oxygen and sulfur isotope geochemistry revealing a significant crustal signature in the genesis of the post-collisional granitoids in central Anatolia. J Asian Earth Sci 30: 403-416.

Boztuğ D, Arehart GB, Platevoet B, Harlavan Y, Bonin B 2007. High-K, calc-alkaline I-type granitoids from the composite Yozgat batholith generated in a post-collisional setting following continent-oceanic island arc collision in central Anatolia, Turkey. Mineralogy and Petrology 91: 191-223.

Boztuğ D, Harlavan Y (2008). K-Ar ages of granitoids unravel the stages of Neo-Tethyan convergence in the eastern Pontides and central Anatolia, Turkey. Int J Earth Sci 97: 585-599.

Boztuğ D, Jonckheere RC, Heizler M, Ratschbacher L, Harlavan Y, Tichomirova M (2009). Timing of post-obduction granitoids from intrusion through cooling to exhumation in central Anatolia, Turkey. Tectonophysics 473: 223-233.

Çakır O, Erduran M (2011). On the P and S receiver functions used for inverting the one-dimensional Upper Mantle shear-wave velocities. Surv Geophys 32: 71-98.

El-Nabi SHA (2012). Curie point depth beneath the Barramiya-Red Sea coast area estimated from spectral analysis of aeromagnetic data. J Asian Earth Sci 43: 254-266.

Erişen B, Akkuş I, Uygur N, Koçak A (1996). Turkiye Jeotermal Envanteri. Maden Tetkik ve Arama Genel Müdürlüğü (in Turkish).

Erler, A Göncüoglu, M C, (1996). Geologic and tectonic setting of the Yozgat batholith, Northern Central Anatolian Crystalline Complex, Turkey. International Geology Review, 38: 714-726.

Göncüoğlu, M C, Toprak, V, Kuscu, İ, Erler, A, Olgun, E (1991). Geology of the western part of the Central Anatolian Massif, Part 1: Southern Section. Turkish Petroleum Company Report (in Turkish) Unpubl. Report No.2909.

Hsieh HH, Chen CH, Lin PY, Yen HY (2014). Curie point depth from spectral analysis of magnetic data in Taiwan. J Asian Earth Sci 90: 26-33.

Hunt CP, Moskowitz BM, Banerjee SK (1995). Magnetic properties of rocks and minerals. In: Ahrens TJ, editor. Rock Physics and Phase Relations: a Handbook of Physical Constants. Washington, DC, USA: American Geophysical Union.

Karastathis VK, Papoulia J, Di Fiore B, Makris J, Tsambas A, Stampolidis A, Papadopoulos GA, 2011. Deep structure investigations of the geothermal field of the North Euboean Gulf, Greece, using 3-D local earthquake tomography and Curie point depth analysis. J Volcanol Geotherm Res 206: 106-120.

Kind R, Eken T, Tilmann F, Sodoudi F, Taymaz T, Bulut F, Yuan X, Can B, Schneider F (2015). Thickness of the lithosphere beneath Turkey and surroundings from S-receiver functions. Solid Earth 6: 971-984.

Lefebvre C, Meijers MJM, Kaymakcı N, Peynircioğlu A, Langereis CG, van Hinsbergen DJJ (2013). Reconstructing the geometry of central Anatolia during the late Cretaceous. Large-scale Cenozoic rotations and deformation between the Pontides and Taurides. Earth Planet Sci Lett 366: 83-98.

Maden N, Aydın A, Kadirov F (2015). Determination of the crustal and thermal structure of the Erzurum-Horasan-Pasinler basins (eastern Türkiye) using gravity and magnetic data. Pure Appl Geophys 172: 1599-1614.

Mayhew MA (1982). Application of satellite magnetic anomaly data to Curie Isotherm Mapping. J Geophys Res 87: 4846-4854.

Nwogbo PO (1998). Spectral prediction of magnetic sources depths from simple numerical models. Comp Geosci 24: 847-852.

Obande GE, Lawal KM, Ahmed LA (2014). Spectral analysis of aeromagnetic data for geothermal investigation of Wikki Warm Spring, North-east Nigeria. Geothermics 50: 85-90.

Okubo Y, Graf RJ, Hansen RO, Ogawa K, Tsu H (1985). Cruie point depths of the island of Kyushu and surrounding areas, Japan. Geophysics 50: 481-494.

Okubo Y, Tsu H, Ogawa K (1989). Estimation of Curie point and geothermal structure of island arcs of Japan. Tectonophysics 159: 279-290.

Piper JDA (1987). Paleomagnetism and the Continental Crust. New York, NY, USA: Wiley.

Ram Babu HV (1997). Average crustal density of the Indian lithosphere-an inference from gravity anomalies and deep seismic soundings. J Geodyn 23: 1-4.

Riad S, Refai E, Ghalib M (1981). Bouguer anomalies and crustal structure in the Eastern Mediterranean. Tectonophysics 71: 253-266.

Rivero L, Pinto V, Casas A (2002). Moho depth structure of the eastern part of the Pyrenean belt derived from gravity data. J Geodyn 33: 315-332.

Roest WR, Verhoef J, Pilkington M (1992). Magnetic interpretation using the 3D analytic signal. Geophysics 57: 116-125.

Saunders P, Priestley K, Taymaz T (1998). Variations in the crustal structure beneath western Turkey. Geophys J Int 134: 373-389.

Şengör AMC, Yılmaz Y (1981). Tethyan evolution of Turkey: a plate tectonic approach. Tectonophysics 75: 181-241.

Springer M (1999). Interpretation of heat-flow density in the Central Andes. Tectonophysics 306: 377-395.

Tezel T, Shibutani T, Kaypak B (2013). Crustal thickness of Turkey determined by receiver function. J Asian Earth Sci 75: 36-45.

Tsokas GN, Hansen RO, Fytikas M (1998). Curie point depth of the island of Crete (Greece). Pure Appl Geophys 152: 747-757.

Turcotte DL, Schubert G (1982). Geodynamics: Applications of Continuum Physics to Geological Problems. New York, NY, USA: Wiley.

Woolard GP (1959). Crustal structure from gravity and seismic measurements. J Geophys Res 64: 1524-1544.